Veterinary Pathology
2023, Vol. 60(1) 52–59

DOI: 10.1177/03009858221131363
journals.sagepub.com/home/vet


Utility of fluorescence imitating brightfield imaging microscopy for the diagnosis of feline chronic enteropathy

Sarah Au Yeung[1], Paula Giaretta[2], Taryn Morningstar[3], Eduardo Masuda[4], Maria Questa[1], Farzad Fereidouni[3], Richard M. Levenson[3], and Sina Marsilio[1]

Abstract

Fluorescence imitating brightfield imaging (FIBI) is a novel microscopy method that allows for real-time, nondestructive, slide-free tissue imaging of fresh, formalin-fixed, or paraffin-embedded tissue. The nondestructive nature of the technology permits tissue preservation for downstream analyses. The objective of this observational study was to assess the utility of FIBI compared with conventional hematoxylin and eosin (H&E)-stained histology slides in feline gastrointestinal histopathology. Formalin-fixed paraffin-embedded full-thickness small intestinal tissue specimens from 50 cases of feline chronic enteropathy were evaluated. The ability of FIBI to evaluate predetermined morphological features (epithelium, villi, crypts, lacteals, fibrosis, submucosa, and muscularis propria) and inflammatory cells was assessed on a 3-point scale (0 = FIBI cannot identify the feature; 1 = FIBI can identify the feature; 2 = FIBI can identify the feature with more certainty than H&E). H&E and FIBI images were also scored according to World Small Animal Veterinary Association (WSAVA) Gastrointestinal Standardization Group guidelines. FIBI identified morphological features with similar or, in some cases, higher confidence compared with H&E images. The identification of inflammatory cells was less consistent. FIBI and H&E images showed an overall poor agreement with regard to the assigned WSAVA scores. While FIBI showed an equal or better ability to identify morphological features in intestinal biopsies, its ability to identify inflammatory cells is currently inferior compared with H&E-based imaging. Future studies on the utility of FIBI as a diagnostic tool for noninflammatory histopathologic lesions are warranted.

Keywords

cat, feline, feline chronic enteropathy, fluorescence imitating brightfield imaging, inflammatory bowel disease, low-grade intestinal T-cell lymphoma, lymphocytic-plasmacytic enteritis

Feline chronic enteropathy (FCE) is among the most common disorders in the elderly cat population, with rising incidence over the past decades. The disorder comprised mostly lymphocytic-plasmacytic enteritis (LPE) and low-grade intestinal T-cell lymphoma (LGITL).[1,25,26,31,32,34] The histopathologic examination of hematoxylin and eosin (H&E)-stained biopsy specimens is considered to be the gold standard for the diagnosis and differentiation of chronic enteropathies.[29] However, the preparation of conventional H&E slides is expensive and time- and resource-consuming.[14,21,22,27,28,33] In addition, formalin fixation often interferes with or even prevents downstream analyses such as flow cytometry and mass spectrometry.[3]

In recent years, various slide-free pathology techniques for rapid evaluation of tissue biopsies without processing and sectioning of paraffin blocks have been developed. Approaches include confocal microscopy,[19] light-sheet microscopy,[16] nonlinear microscopy (ie, multiphoton and stimulated Raman scattering),[15,37] and microscopy with ultraviolet surface excitation (MUSE).[12,24] Compared with current tissue processing and slide generation methods, which require approximately 10 to 12 hours to complete, slide-free pathology methods could greatly improve the speed of diagnosis, reduce cost, and conserve tissue biopsies for advanced ancillary studies.

Fluorescence imitating brightfield imaging (FIBI) is a novel slide-free imaging modality that allows for nondestructive direct and real-time imaging of thick, unsectioned, fresh, or fixed tissue specimens, making it an attractive alternative imaging method for research samples[12] while outperforming alternative approaches in terms of simplicity, speed, and costs.[13] FIBI is based on the use of absorbing stains, applied directly on the tissue surface, coupled with illumination at 405 nm using an epifluorescence light path. The 405-nm excitation light generates broad-spectrum autofluorescence diffusely inside the thick, unsectioned tissue. This autofluorescence then back-illuminates through a surface-stained layer to generate a superficial

[1]UC Davis School of Veterinary Medicine, Davis, CA
[2]Universidade Federal de Minas Gerais, Belo Horizonte, Brazil
[3]UC Davis Health, Sacramento, CA
[4]Axys Análises, Porto Alegre, Brazil

Supplemental Material for this article is available online.

Corresponding Author:
Sina Marsilio, Department of Medicine and Epidemiology, UC Davis School of Veterinary Medicine, 1275 Med Science Drive, Davis, CA 95616, USA.
Email: smarsilio@ucdavis.edu

image of the tissue's cellular morphology. Conveniently, the stains that work well in this application are the familiar H&E reagents. As in conventional slide-based histology, hematoxylin is a strongly absorbing and nonfluorescing dye that binds predominantly to nuclei. Eosin staining provides a red-pink tint to protein and some nuclear components while also contributing additional contrast in FIBI images due to its intrinsic fluorescence.[23] In clinical practice, FIBI could be used intraoperatively to help guide decision making or be used for real-time diagnosis to determine an accurate prognosis and optimal treatment plan. A validation study evaluating the diagnostic concordance of FIBI images compared with conventional H&E assessment on a wide array of human tissues including breast, bladder, and gastrointestinal tissue, with diagnosis varying from normal/benign, cancer, and noncancerous origins, reported a concordance of 97.0%.[6]

This observational, proof-of-concept study aimed to evaluate the diagnostic utility of FIBI for the pathological assessment of formalin-fixed paraffin-embedded (FFPE) intestinal tissue biopsies from cats with FCE. We hypothesized that FIBI is an efficient, affordable, and reliable diagnostic tool for the diagnosis and differentiation of FCE.

Materials and Methods

Sample Selection and Preparation

For this proof-of-concept observational study, the tissue archive of a commercial pathology laboratory (Axys Análises Laboratório, Porto Alegre, Brasil) was searched for FFPE small intestinal tissue biopsy specimens from cats with suspected chronic enteropathy. Fifty archived tissue blocks with biopsy specimens of sufficient post-diagnostic size and orientation were identified and shipped to the UC Davis Veterinary Teaching Hospital for further analysis. Conventional H&E slides of approximately 4 µm were prepared, scanned with a 20× objective slide scanner (Aperio AT2 DX System; Leica Biosystems, Nussloch, Germany), and uploaded on a web-based histological platform (Aperio ImageScope™ version 12.4.3; Leica Biosystems) for histological assessment.

Fluorescence Imitating Brightfield Imaging

Tissue blocks underwent surface deparaffinization (affecting only about the top 100 µm of the block) with serial washes using pure xylene dropwise and 95% ethanol. Serial washes were repeated until the embedded tissue surface was cleared of wax while the majority of the tissue specimen remained embedded in the block. The tissue surface was stained using Mayer's hematoxylin for 30 seconds, washed for 10 seconds with deionized water, and counterstained with eosin for 30 seconds. Blocks were placed on a custom imaging cassette and illuminated using a 405-nm LED light (LZ1-00UB00, LED Engin). A 10× objective (Nikon, Japan) was used to collect images with 9-megapixel scientific-grade CCD color camera (Ximea, MDO901CU-SY, Münster, Germany) connected via a 160-mm tube lens (Thorlabs TTL 165-A; Thorlabs Inc., Newton, New Jersey) (Fig. 1). Multiple raster-scanned images of the tissue areas were captured by the FIBI microscope camera. Images were stitched to create a single image of the entire biopsy specimen using a stitching program (Microsoft Image Composite Editor version 2.0). To have the same brightness and color density among all the images, FIBI images were brightened and sharpened using an open-source digital imaging editing program (GIMP version 2.10.30).

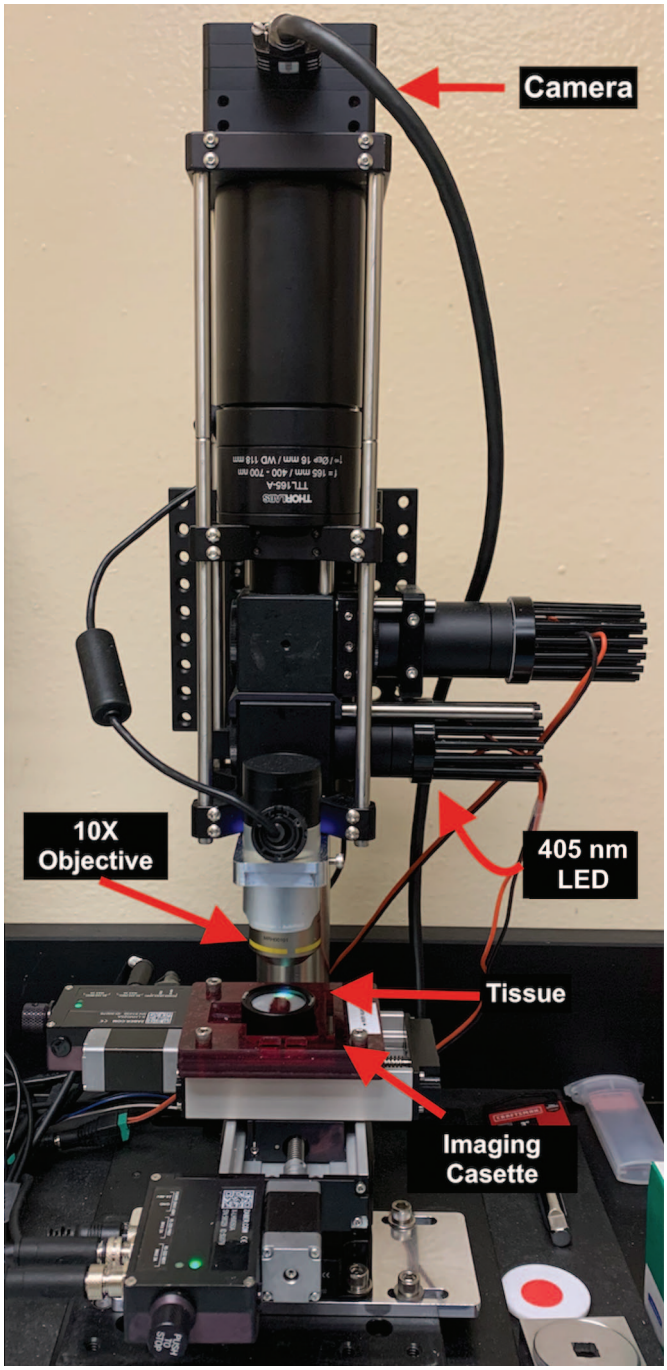

Figure 1. Fluorescence imitating brightfield imaging (FIBI) microscope setup. A light-emitting 405-nm (blue) LED light excites the stained tissue surface. The excited light is collected by 10× objective and camera.

Evaluation of Diagnostic Concordance Between H&E Images and FIBI-Generated Images

Digital H&E images were assessed without provision of clinical data by a single board-certified veterinary pathologist (P. Giaretta) and scored according to the published guidelines by the World Small Animal Veterinary Association (WSAVA) Gastrointestinal Standardization Group.[11,35] After an 8-week washout period, images of the biopsy specimens generated by FIBI were assessed by the same pathologist and scored according to the above-mentioned guidelines.

Following the WSAVA scoring of the biopsy specimens using H&E and FIBI images, predetermined anatomical structures and inflammatory cells were evaluated to determine the diagnostic concordance between FIBI and H&E images using a 3-point scoring scheme (0 = FIBI cannot identify the structure without correlating with H&E; 1 = FIBI can identify the structure without the need of H&E; 2 = FIBI can identify the structure with more certainty than H&E). Predetermined anatomical structures included mucosal structures as defined by WSAVA guidelines as well as blood vessels and ganglia in the submucosa and muscularis (Table 1).

The average total and subscores were calculated by adding individual total or subscores of all 44 cases, respectively, and dividing the sum by the number of cases. Subscores were used to determine how well FIBI could identify inflammation compared with morphological features in the mucosa. Furthermore, subscores were calculated for each layer to determine how well FIBI can identify structures in the mucosa, submucosa, and muscularis. See Supplemental Tables S1–S5 (online version) for individual WSAVA scores and correlation scores.

Table 1. Average FIBI scores for the identification of predetermined anatomical structures on 44 formalin-fixed paraffin-embedded tissue samples based on a 3-point scale (0 = FIBI cannot identify the structure without correlating with H&E; 1 = FIBI can identify the structure without the need of H&E; 2 = FIBI can identify the structure with more certainty than H&E).

Mucosal Structure	Score
Morphological features	
Epithelium and epithelial injury	0.93
Villi and villous stunting	1.96
Crypts and crypt dilation/distortion	0.91
Lacteals and lacteal dilation	0.02
Mucosal fibrosis	0.40
Subscore—Mucosal morphological features	**0.84**
Inflammation	
Intraepithelial lymphocytes	0.10
LP infiltrating cells	0.66
LP lymphocytes and plasma cells	0.05
LP eosinophils	0
LP neutrophils	0.15
LP macrophages	0.45
Subscore—Mucosal inflammation	**0.24**
Total mucosal score	**0.51**
Blood vessels in the submucosa	0.98
Submucosa infiltrating cells	0.93
Submucosa ganglia	1
Subscore—Submucosa	**0.97**
Blood vessels in muscularis externa	0.98
Muscularis mucosa infiltrating cells	1
Muscularis externa infiltrating cells	0.93
Muscularis externa ganglia	0.95
Muscularis externa thickness	0.94
Subscore—Muscularis	0.96
Sum	12.36/18
Total full-thickness score	**0.69**
Total inflammation score	**0.48**

Abbreviations: FIBI, fluorescence imitating brightfield imaging; LP, lamina propria.

Statistical Analysis

Limits of agreement for the histopathologic assessment based on WSAVA scorings of images generated by FIBI compared with conventional H&E images were calculated by Bland-Altman analysis.[2] Values are given as mean (95% confidence interval). Correlation between the 2 methods for WSAVA scoring was calculated using the Spearman correlation where correlation coefficients of <0.39 were considered weak; 0.40–0.69, moderate; 0.70–0.89, strong; and >0.90, very strong. All statistical analyses were performed using GraphPad Prism version 9.3.1 for macOS (GraphPad Software, San Diego, California).

Results

Study Population and Image Acquisition Using FIBI

Of the 50 samples evaluated by H&E, 44 biopsy specimens (30 jejunum, 4 ileum, 2 duodenum, and 8 from ≥2 sections of small intestine) were deemed appropriate for further assessment with FIBI. Four samples were rated as insufficient for evaluation due to poor tissue orientation and 2 samples had no significant findings on the initial H&E evaluation. Biopsy specimens were from 27 mixed breed, 12 Persians, 1 Bengal, 1 British Shorthair, 1 Himalayan, 1 Siamese, and 1 cat of unknown breed and had an average age of 7.97 years (range: 1–16 years, 22 cats reported of unknown age). Clinical signs were reported for 38 of 44 cats and included intestinal wall thickening (68.2% [30/44]), vomiting (56.8% [25/44]), progressive weight loss/emaciation (20.5% [9/44]), chronic diarrhea (9.1% [4/44]), and/or enlarged mesenteric lymph nodes (6.8% [3/44]) (Supplemental Table S6).

Based on conventional H&E evaluation, 12 cases were diagnosed with LGITL, 24 with inflammatory bowel disease (5 with neutrophilic enteritis, 2 with eosinophilic enteritis, 5 with LPE, 4 with neutrophilic and eosinophilic enteritis, 3 with neutrophilic and lymphoplasmacytic enteritis, 1 with lymphocytic-plasmacytic and eosinophilic enteritis, 2 with lymphocytic-plasmacytic, eosinophilic, and neutrophilic enteritis, 1 with ulcerative enteritis, and 1 with mural granulomatous inflammation), 5 were not able to be differentiated between LGITL and LPE, 1 with large cell lymphoma, and 2 with only fibrosis present.

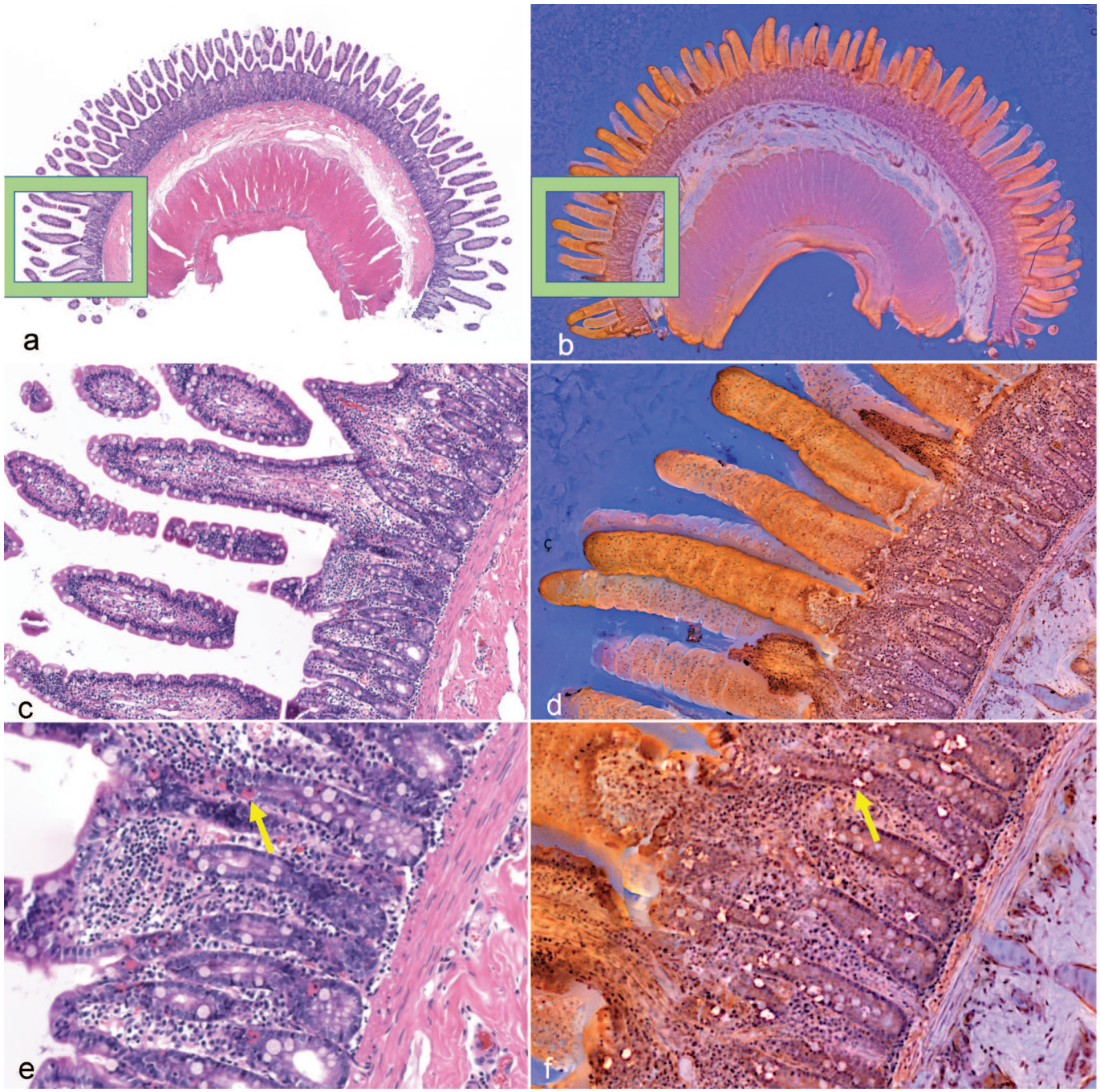

Figure 2. Multifocal eosinophilic and neutrophilic enteritis, jejunum, cat. Comparison of conventional light microscopy (a, c, e) with fluorescence imitating brightfield imaging (FIBI) (b, d, f). (a, c, e) Conventional light microscopy images reveal eosinophil and neutrophil infiltration in the lamina propria. Occasionally, intraepithelial lymphocyte numbers appear increased. (b, d, f) FIBI images demonstrate unsectioned villi in 3 dimensions with only epithelial cells and goblet cells visualized. FIBI identified morphological features, but was unable to reliably differentiate inflammatory cells, fibrosis, and lacteals (d, f) within the mucosa without guidance provided by the corresponding H&E slide. Globular leukocytes are fluorescent and abundant in FIBI images compared with conventional light field microscopy (yellow arrows).

The average time needed to acquire each FIBI image was approximately 30 minutes including approximately 15 minutes for deparaffinization and staining and 15 minutes for image acquisition and editing. This compares favorably to the standard of time, approximately 10 to 12 hours, for processing H&E slides. However, interpretation of FIBI-acquired images was reported to be more time-consuming by the evaluator, which was mostly attributed to unfamiliarity with the FIBI images compared with conventional H&E images (Fig. 2).

Ability of FIBI to Identify Predetermined Mucosal Structures and Lesions

Assessment of the ability of FIBI to identify predetermined mucosal structures resulted in an average score of 0.51,

demonstrating a weaker ability to identify mucosal lesions compared with H&E images and inferiority to conventional H&E slides. Comparing subscores for morphological and inflammatory features, the weak overall score was mostly driven by poor identification of inflammatory cells in FIBI images (subscore of 0.24). On average, identification of the majority of architectural morphological features and lesions by FIBI was comparable to conventional H&E (surface epithelium, crypt dilation/distortion, blood vessels, ganglia, and thickness of muscularis externa) (subscore of 0.90). FIBI was superior to H&E in the evaluation of villi and villous stunting (average score of 1.96). FIBI was able to identify structures and infiltrating cells in the submucosa (subscore of 0.97) and muscularis (subscore of 0.96) at approximately the same ability as traditional H&E slides. Overall, although the histological morphology was generally well identified, FIBI analysis did not reliably differentiate inflammatory cells, fibrosis, or lacteals within the mucosa without guidance provided by the corresponding H&E slide.

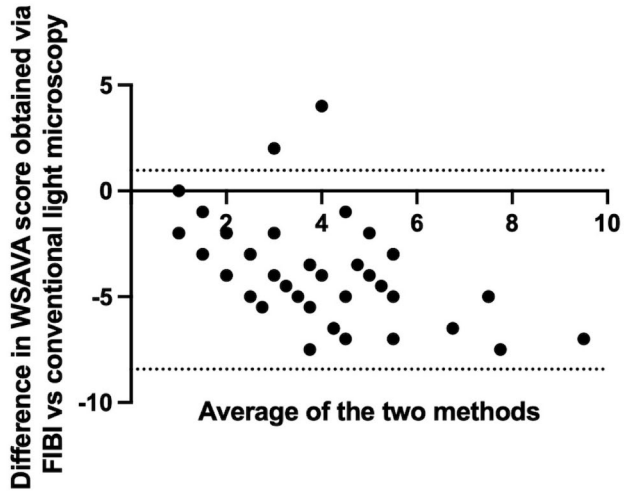

Figure 3. Bland-Altman plots showing bias (mean of differences) for the World Small Animal Veterinary Association (WSAVA) score obtained via FIBI analysis vs conventional H&E. The mean bias was −3.73 (SD 2.40). Dashed lines represent the 95% limits of agreement. FIBI, fluorescence imitating brightfield imaging.

Histopathologic Concordance Between H&E Images and FIBI-Generated Images

The Bland-Altman plot is a graphical method to compare 2 measurement techniques.[4,5] In the graph, the differences between the 2 techniques (x-axis) are plotted against the averages of the 2 techniques (y-axis). The Bland-Altman plot in Fig. 3 compares the WSAVA score obtained via FIBI with the WSAVA score obtained via conventional light microscopy. The graph illustrates that FIBI systematically underestimates the WSAVA score compared with conventional light microscopy.

There was substantial bias of the WSAVA scoring (Supplemental Table S3) between conventional H&E images and FIBI-based images (−3.73; 95% limits of agreement: −8.42 to 0.97) (Fig. 3). Correlation between FIBI-based and H&E-based scoring was moderate with a correlation coefficient of 0.47 (95% confidence interval: 0.18–0.68). See online version of the manuscript for supplemental materials of individual WSAVA scores.

Discussion

To our knowledge, this is the first study to investigate FIBI microscopy for the evaluation and diagnosis of FCE. Slide-free histopathology is a growing area of research due to the need for more efficient and inexpensive tissue evaluation in veterinary and human medicine. While there are other slide-free methodologies currently or previously being investigated, FIBI microscopy is simpler and cheaper than other technologies. For example, conventional light-sheet fluorescence microscopy requires nonstandard and often difficult sample preparation for clearing of tissue samples, complicating the workflow of a routine clinical procedure,[16,24] compared with FIBI that only needs brief staining of the tissue surface to image. Common goals shared among all slide-free histopathology modalities are to provide imaging that is real-time, nondestructive, and of high diagnostic quality.[12,13,16,17,24,30] An additional benefit FIBI provides is its ability to capture surface topography, as shown in this study by the high-quality rendition of intact intestinal villi and an average score of 1.96 from FIBI images compared with H&E, which may prove to have clinical utility once this capability is more fully explored. FIBI could have a wide range of clinical applications including postoperative evaluation and triage of surgical biopsy specimens (ie, selecting the most representative or diagnostic sections of a biopsy to improve conventional H&E imaging), intraoperative assessment of tumor-margin surfaces, and intraoperative imaging and fluorescence-guided surgery using systemically administered contrast agents.[12,13,16] While the diagnosis of chronic conditions including chronic enteropathies is usually not considered urgent, the technology allows for tissue preservation for downstream analysis of the same tissue that was imaged and may be particularly interesting in investigative studies, given that most gastrointestinal samples are small endoscopic biopsies.

In this study, FIBI allowed for (or enabled) the identification of many morphological structures with an accuracy that approximates or is superior to that of conventional H&E microscopy at a fraction of the time of traditional H&E slide preparation. Villi and villous stunting were identified with more confidence in the FIBI images than in the conventional H&E slides, which is a feature scored by WSAVA guidelines based on the severity of the lesion.[11,35] Other structures that were identified at approximately the same confidence as conventional H&E slides included the epithelium and epithelial injury, crypts and crypt dilation, blood vessels, ganglia, infiltrating cells in the submucosa and muscularis, and muscularis externa thickness. While the histological morphology of the small intestine was generally well defined in FIBI images, FIBI

did not allow for reliable differentiation of inflammatory cells, fibrosis, or lacteals within the mucosa without guidance provided by the corresponding H&E slide. This was in part because the surface of the uncut tissue was imaged directly, and thus FIBI images often showed the external surface of the villi in a 3-dimensional aspect (only epithelial cells and goblet cells visualized) rather than a transverse cut into the villi (Fig. 2). This limited the ability for the pathologist to examine intraepithelial lymphocytes, lacteals, and the amount of cellular infiltration located in the lamina propria. This was a major limitation as epitheliotropism (especially the formation of intraepithelial nests and plaques) and the quantity and type of cellular infiltration are important histological features to differentiate between LPE and LGITL in feline intestinal biopsy samples.[11,20,35] Another possible explanation for the limited ability to identify inflammatory cells may be that image scans shown here were acquired using a 10× objective, due to currently limited computational power. However, we are currently working on scans using 20× (or higher) objectives. A previous study investigating the utility of a similar predecessor technology to FIBI, MUSE, in human dermatopathology found similar results.[30] While MUSE images were able to identify morphological features in the skin such as collagen, elastin, adipose tissue, nerves, vasculature, sweat glands, stratum corneum, and stratum spinosum at equal or improved ability to conventional H&E, the identification of inflammatory cells was inferior to traditional H&E.[30] In another preliminary validation study for MUSE that evaluated benign and malignant neoplasms in multiple tissue types, MUSE accurately diagnosed 93% of cases compared with the conventional H&E diagnosis[12] and accurately diagnosed basal cell carcinoma and pseudoxanthoma elasticum in abnormal skin samples.[30]

While the WSAVA histopathological guidelines focus on lesions in the mucosa, the ability to see infiltrating cells and muscularis layer in the FIBI images is important for differentiating LGITL from LPE in full-thickness specimens.[20] Also, the ability to see structures such as blood vessels and ganglia with the same (or better) resolution and tissue contrast than provided by H&E may be helpful for the diagnosis of ganglionopathies or aganglionosis in people and animals (ie, Hirschsprung disease or lethal white overo syndrome).[7]

Cats with chronic enteropathy frequently show an ultrasonographically thickened muscularis layer of the small intestinal tract.[10,38] A recent study found that the presence of ultrasonographic lesions within the submucosal and muscularis layers was not predictive of histological lesions in those layers in a population of cats with a high prevalence of chronic enteropathy.[18] However, as this was a retrospective study on FFPE tissue, shrinkage artifacts cannot be excluded and may have led to a lack of correlation between ultrasonographic and histopathologic findings. Formalin commonly causes tissue shrinkage, with shrinkages rates between 28% and 31% in gastric and small intestinal biopsy specimens being reported in humans and dogs, respectively.[8,9] FIBI allows for imaging of unfixed tissue, and results of this study show an overall good ability of FIBI to identify morphological features present in the submucosa and muscularis layers. Therefore, FIBI may be a valuable tool for future studies investigating the relationship between ultrasonographic findings in the submucosa and muscularis layer and histopathologic changes in cats with chronic enteropathy.

This study showed an overall poor agreement between the WSAVA scores assessed by FIBI versus conventional H&E imaging. This was again mostly driven by the limited ability of FIBI to identify inflammatory cells in the uncut villi and the mucosa, and thus FIBI showed a general bias toward underestimating the WSAVA score. This theory is underscored by the fact that inflammatory cells in the submucosa and muscularis were easily identified, which is reflected in the higher score (0.93) compared with the lamina propria (0.24). This is in contrast to a previous study in which FIBI demonstrated an accuracy of 97% compared with the diagnosis made on H&E slides in a variety of fixed human tissue specimens. In that study, minor discordances (defined as alternative diagnoses without clinical treatment or outcome implications) were slightly higher in FIBI images (7.2%) compared with H&E slides (5.0%). Major discordance, defined as a different diagnosis that would lead to a different treatment recommendation/outcome, was 3.0% for FIBI images compared with conventional H&E slides, which was 1.2%. The tissue biopsies included in the preliminary study originated from the bladder, larynx, endocrine, breast, reproductive, gastrointestinal, and soft tissues with diagnoses including normal, hyperplasia, benign neoplasms, cancers, and inflammatory lesions.[6] Future studies are needed to evaluate and validate the utility of FIBI for neoplastic and noninflammatory lesions.

This study has several limitations. While FIBI's highest potential applicability in the preclinical and clinical fields is with the use of fresh tissue specimens, this proof-of-concept study used archived FFPE full-thickness tissue specimens. Therefore, we do not know whether the results of this study will translate directly to fresh and frozen tissue or endoscopic biopsies. However, the use of fresh tissue biopsies would have required a prospective study set-up where patient enrollment usually takes time and requires ethical approval. Results for this study may still serve as a solid basis and guidance for future prospective studies. Another limitation of the study is the unfamiliarity of the pathologist to the fluorescent coloration of FIBI images. Future developments may allow for FIBI images to be color-remapped into virtual H&E stains, which may improve readability. FIBI also has the potential to be integrated with artificial intelligence technology to easily convert FIBI images to traditional H&E coloration or mimic other special stains, which may potentially overcome this limitation.[12,24,30] Finally, we had only a single pathologist assessing the histology for this study. Substantial interobserver variability for the assessment of small animal gastrointestinal biopsies has previously been reported.[36] However, assessment of interobserver variability was outside the scope of this study. Hence, we do not believe this would have added to the body of knowledge gained from this study.

In conclusion, this study showed that FIBI can successfully identify most morphological features and morphological

lesions in the feline intestine with limited differentiation between inflammatory cells. While FIBI microscopy does not currently replace conventional H&E sections for the evaluation of gastrointestinal inflammatory lesions, further studies on FIBI's utility for noninflammatory and neoplastic lesions are warranted, as well as a focus on technical developments to improve performance on inflammatory lesions.

Acknowledgments

We thank the Students Training in Advanced Research (STAR) Program at the University of California, Davis for financial support on this project.

Declaration of Conflicting Interests

The author(s) declared the following potential conflicts of interest with respect to the research, authorship, and/or publication of this article: Dr Richard M. Levenson and Dr Farzad Fereidouni are co-founders of Histolix Inc.; the remaining authors have stated that they have no conflict of interest.

Funding

The author(s) disclosed receipt of the following financial support for the research, authorship, and/or publication of this article: Sarah Au Yeung received funding from the Students Training in Advanced Research (STAR) Program at the University of California, Davis.

ORCID iDs

Sarah Au Yeung https://orcid.org/0000-0003-4418-078X
Sina Marsilio https://orcid.org/0000-0002-0693-0669

References

1. Al-Ghazlat S, de Rezende CE, Ferreri J. Feline small cell lymphosarcoma versus inflammatory bowel disease: diagnostic challenges. *Compend Contin Educ Vet*. 2013;**35**:E1–E5; quiz E6.
2. Altman DG, Bland JM. Measurement in medicine: the analysis of method comparison studies. *J Roy Stat Soc D: Sta*. 1983;**32**:307–317.
3. Atwood J, Neumann D, Dammer E, et al. Evaluating the effect of formalin fixation on mass spectrometry-based proteomic profiling (984.1). *FASEB J*. 2014;**28**:984.1.
4. Bland JM, Altman DG. Comparing methods of measurement: why plotting difference against standard method is misleading. *Lancet*. 1995;**346**:1085–1087.
5. Bland JM, Altman DG. Measuring agreement in method comparison studies. *Stat Methods Med Res*. 1999;**8**:135–160.
6. Borowsky AD, Levenson RM, Gown AM, et al. A pilot validation study comparing FIBI, a slide-free imaging method, with standard FFPE H&E tissue section histology for primary surgical pathology diagnosis. *medRxiv*. Published 2022. Accessed October 3, 2022. https://www.medrxiv.org/content/10.1101/2022.03.10.22272226v1.
7. Butler Tjaden NE, Trainor PA. The developmental etiology and pathogenesis of Hirschsprung disease. *Transl Res*. 2013;**162**:1–15.
8. Ciyiltepe H, Ergin A, Somay A, et al. The effects of formalin solution on wall thickness and size in stomach resection materials. *Bosphorus Med J*. 2021;**8**(1):41–46.
9. Clarke BS, Banks TA, Findji L. Quantification of tissue shrinkage in canine small intestinal specimens after resection and fixation. *Can J Vet Res*. 2014;**78**:46–49.
10. Daniaux LA, Laurenson MP, Marks SL, et al. Ultrasonographic thickening of the muscularis propria in feline small intestinal small cell T-cell lymphoma and inflammatory bowel disease. *J Feline Med Surg*. 2014;**16**:89–98.
11. Day MJ, Bilzer T, Mansell J, et al. Histopathological standards for the diagnosis of gastrointestinal inflammation in endoscopic biopsy samples from the dog and cat: a report from the World Small Animal Veterinary Association Gastrointestinal Standardization Group. *J Comp Pathol*. 2008;**138**(suppl 1):S1–S43.
12. Fereidouni F, Harmany ZT, Tian M, et al. Microscopy with ultraviolet surface excitation for rapid slide-free histology. *Nat Biomed Eng*. 2017;**1**:957–966.
13. Fereidouni F, Levenson RM. Fluorescence imitating brightfield imaging. Published 2020. Accessed October 3, 2022. https://patentscope.wipo.int/search/en/detail.jsf?docId=WO2021067726.
14. Freiche V, Paulin MV, Cordonnier N, et al. Histopathologic, phenotypic, and molecular criteria to discriminate low-grade intestinal T-cell lymphoma in cats from lymphoplasmacytic enteritis. *J Vet Intern Med*. 2021;**35**:2673–2684.
15. Freudiger CW, Min W, Saar BG, et al. Label-free biomedical imaging with high sensitivity by stimulated Raman scattering microscopy. *Science*. 2008;**322**:1857–1861.
16. Glaser AK, Reder NP, Chen Y, et al. Light-sheet microscopy for slide-free non-destructive pathology of large clinical specimens. *Nat Biomed Eng*. 2017;**1**:0084.
17. Guo J, Artur C, Womack T, et al. Multiplex protein-specific microscopy with ultraviolet surface excitation. *Biomed Opt Express*. 2020;**11**:99–108.
18. Guttin T, Walsh A, Durham AC, et al. Ability of ultrasonography to predict the presence and location of histologic lesions in the small intestine of cats. *J Vet Intern Med*. 2019;**33**:1278–1285.
19. Kiesslich R, Goetz M, Neurath MF. Confocal laser endomicroscopy for gastrointestinal diseases. *Gastrointest Endosc Clin N Am*. 2008;**18**:451–466, viii.
20. Kiupel M, Smedley RC, Pfent C, et al. Diagnostic algorithm to differentiate lymphoma from inflammation in feline small intestinal biopsy samples. *Vet Pathol*. 2011;**48**:212–222.
21. Kokovic I, Novakovic BJ, Cerkovnik P, et al. Clonality analysis of lymphoid proliferations using the BIOMED-2 clonality assays: a single institution experience. *Radiol Oncol*. 2014;**48**:155–162.
22. Langerak AW, Groenen PJ, Bruggemann M, et al. EuroClonality/BIOMED-2 guidelines for interpretation and reporting of Ig/TCR clonality testing in suspected lymphoproliferations. *Leukemia*. 2012;**26**:2159–2171.
23. Lev R, Stoward PJ. On the use of eosin as a fluorescent dye to demonstrate mucous cells and other structures in tissue sections. *Histochemie*. 1969;**20**:363–377.
24. Liu Y, Levenson RM, Jenkins MW. Slide over: advances in slide-free optical microscopy as drivers of diagnostic pathology. *Am J Pathol*. 2021;**192**(2):180–194.
25. Louwerens M, London CA, Pedersen NC, et al. Feline lymphoma in the post-feline leukemia virus era. *J Vet Intern Med*. 2005;**19**:329–335.
26. Marsilio S. Differentiating inflammatory bowel disease from alimentary lymphoma in cats: does it matter? *Vet Clin North Am Small Anim Pract*. 2021;**51**(1):93–109.
27. Marsilio S, Ackermann MR, Lidbury JA, et al. Results of histopathology, immunohistochemistry, and molecular clonality testing of small intestinal biopsy specimens from clinically healthy client-owned cats. *J Vet Intern Med*. 2019;**33**:551–558.
28. Marsilio S, Newman SJ, Estep JS, et al. Differentiation of lymphocytic-plasmacytic enteropathy and small cell lymphoma in cats using histology-guided mass spectrometry. *J Vet Intern Med*. 2020;**34**:669–677.
29. Paulin MV, Couronne L, Beguin J, et al. Feline low-grade alimentary lymphoma: an emerging entity and a potential animal model for human disease. *BMC Vet Res*. 2018;**14**:306.
30. Qorbani A, Fereidouni F, Levenson R, et al. Microscopy with ultraviolet surface excitation (MUSE): a novel approach to real-time inexpensive slide-free dermatopathology. *J Cutan Pathol*. 2018;**45**:498–503.
31. Richter KP. Feline gastrointestinal lymphoma. *Vet Clin North Am Small Anim Pract*. 2003;**33**:1083–1098, vii.
32. Sabattini S, Bottero E, Turba ME, et al. Differentiating feline inflammatory bowel disease from alimentary lymphoma in duodenal endoscopic biopsies. *J Small Anim Pract*. 2016;**57**:396–401.
33. van Dongen JJ, Langerak AW, Bruggemann M, et al. Design and standardization of PCR primers and protocols for detection of clonal immunoglobulin and T-cell receptor gene recombinations in suspect lymphoproliferations:

report of the BIOMED-2 Concerted Action BMH4-CT98-3936. *Leukemia*. 2003;**17**:2257–2317.

34. Waly NE, Gruffydd-Jones TJ, Stokes CR, et al. Immunohistochemical diagnosis of alimentary lymphomas and severe intestinal inflammation in cats. *J Comp Pathol*. 2005;**133**:253–260.
35. Washabau RJ, Day MJ, Willard MD, et al. Endoscopic, biopsy, and histopathologic guidelines for the evaluation of gastrointestinal inflammation in companion animals. *J Vet Intern Med*. 2010;**24**:10–26.
36. Willard MD, Jergens AE, Duncan RB, et al. Interobserver variation among histopathologic evaluations of intestinal tissues from dogs and cats. *J Am Vet Med Assoc*. 2002;**220**:1177–1182.
37. Zipfel WR, Williams RM, Webb WW. Nonlinear magic: multiphoton microscopy in the biosciences. *Nat Biotechnol*. 2003;**21**:1369–1377.
38. Zwingenberger AL, Marks SL, Baker TW, et al. Ultrasonographic evaluation of the muscularis propria in cats with diffuse small intestinal lymphoma or inflammatory bowel disease. *J Vet Intern Med*. 2010;**24**:289–292.